

Engineered Biosynthesis of Novel Polyketides from *Streptomyces* Spore Pigment Polyketide Synthases

Tin-Wein Yu,^{†,‡} Yuemao Shen,^{†,§} Robert McDaniel,^{||} Heinz G. Floss,[†] Chaitan Khosla,^{||,⊥} David A. Hopwood,[‡] and Bradley S. Moore^{*,†}

Contribution from the Department of Chemistry, Box 351700, University of Washington, Seattle, Washington 98195-1700, Department of Genetics, John Innes Centre, Norwich NR4 7UH, United Kingdom, and Departments of Chemical Engineering and Chemistry, Stanford University, Stanford, California 94305-5025

Received February 2, 1998

Abstract: A series of 12 recombinants expressing sets of polyketide synthase (PKS) genes from the *whiE* (*Streptomyces coelicolor*), *sch* (*S. halstedii*), and *cur* (*S. curacoi*) spore pigment biosynthetic gene clusters were prepared and shown to produce four groups of novel polyketides. Mixtures of undecaketides and dodecaketides were produced by the minimal PKS alone (TW93b, TW93c, and TW93d) or in the presence of the (unnatural) *act* ketoreductase (KR) (TW94b, TW94c, and TW94d), whereas when the *whiE*-ORFVI cyclase was present, only dodecaketides (TW95a and TW95b) arose, in high yield. This implies that the *whiE* minimal PKS requires an additional subunit (the cyclase) to stabilize the complex between the long nascent polyketide chain and the minimal PKS to ensure that the chain reaches the full 24 carbons. These experiments suggest that the native spore pigment is a C24 molecule with a pentacenequinone structure which is first cyclized C9 to C14. A fourth set of uncharacterized polyketides was produced when the complete set of three *whiE* cyclases was expressed together with the *whiE* minimal PKS. It seems that the cyclases, the products of *whiE*-ORFs II and VII, act in concert with the remainder of the *whiE* PKS subunits to facilitate construction of the nearly complete spore pigment polyketide. Shortened polyketides were additionally produced by the minimal PKS alone (the heptaketide TW93a) and in the presence of the *act* KR (the pentaketide oracetophenone, TW94a). While these polyketides might be derailment products resulting from a promiscuous chain length factor, they could also arise as degradation products from intermediates in the biosynthesis of the structurally related larger polyketides. Finally, the isolation of the same aromatic polyketide products from the recombinants carrying corresponding genes from the *whiE*, *sch*, and *cur* gene clusters suggests that the various spore pigments observed in *Streptomyces* spp. are derived from similar or identical polycyclic aromatic polyketide intermediates.

Introduction

Spore pigmentation in *Streptomyces* spp. depends on the production of polycyclic aromatic polyketides during the maturation of the spores in the aerial mycelium. The first genetic locus involved in *Streptomyces* spore pigmentation to be identified and cloned was *whiE* of *Streptomyces coelicolor*.¹ Mutations in the *whiE* gene cluster abolished or modified spore pigmentation. Analysis of the *whiE* locus revealed a cluster of eight open reading frames (ORFs), *whiE*-ORFI to -ORFVIII (Figure 1). Some of the deduced gene products resembled the protein subunits of polyketide synthases (PKSs), including those for actinorhodin (*act*),² which is also made by this strain. The isolation and structural elucidation of the corresponding spore pigments, however, has been unsuccessful, perhaps because these metabolites polymerize and become covalently bound to macromolecular spore components.

Aromatic polyketides are formed via enzyme-catalyzed cyclizations of highly reactive enzyme-bound linear poly- β -ketoacyl thioesters, which are synthesized by successive Claisen condensations of multiple extender units derived from malonyl-coenzyme A (CoA) with an acyl-CoA starter unit.³ The PKSs for the aromatic class of polyketides in bacteria have a so-called type II organization in which separate protein subunits come together noncovalently to form the complete synthase. The roles of aromatic PKS subunits have been assigned on the basis of sequence comparisons and in vivo functional analysis. Each PKS contains a "minimal" set of three subunits [a β -ketoacyl synthase (KS), a chain length factor (CLF), and an acyl carrier protein (ACP)], which is required for in vivo polyketide biosynthesis (Figure 1).⁴ Additional PKS subunits, including ketoreductases (KR), cyclases (CYC), and aromatases (ARO), are responsible for modification of the nascent chain to form the specific cyclized polyketide product.

A second PKS gene cluster involved in spore pigmentation has been identified in *S. halstedii* (*sch*),⁵ and a third in *S. curacoi* (*cur*)⁶ may play a similar role. The homologous *sch* and *cur*

* Email: bmoore@chem.washington.edu.

[†] University of Washington.

[‡] John Innes Centre.

[§] Permanent address: Laboratory of Phytochemistry, Kunming Institute of Botany, Chinese Academy of Science, Kunming, Yunnan, Peoples Republic of China.

^{||} Department of Chemical Engineering, Stanford University.

[⊥] Department of Chemistry, Stanford University.

(1) Davis, N. K.; Chater, K. F. *Mol. Microbiol.* **1990**, *4*, 1679–1691.

(2) Fernández Moreno, M. A.; Martínez, E.; Boto, L.; Hopwood, D. A.; Malpartida, F. *J. Biol. Chem.* **1992**, *267*, 19278–19290.

(3) O'Hagan, D. *The Polyketide Metabolites*; Ellis Horwood: Chichester, 1991.

(4) Hopwood, D. A. *Chem. Rev.* **1997**, *97*, 2465–2497.

(5) Blanco, G.; Pereda, A.; Méndez, C.; Salas, J. A. *Gene* **1992**, *112*, 67–76.

(6) Bergh, S.; Uhlén, M. *Gene* **1992**, *117*, 131–136.

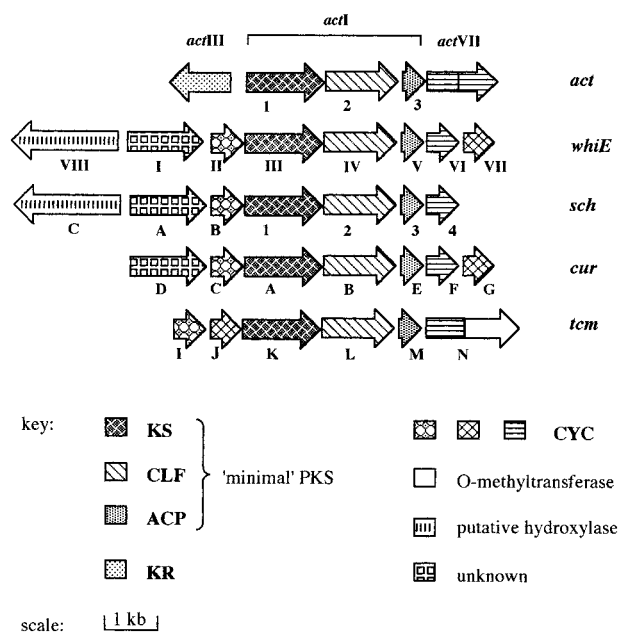


Figure 1. Organization of aromatic PKS biosynthetic gene clusters from *Streptomyces* spp.: actinorhodin (*act*) and the *whiE*-encoded spore pigment from *S. coelicolor*, the *sch*-encoded spore pigment from *S. halstedii*, the *cur*-encoded spore pigment from *S. curacaoi*, and tetracenomycin (*tm*) from *S. glaucescens*. The arrows depict the relative sizes of the genes and are shaded to represent their functions.

gene clusters (Figure 1) are strikingly similar to the *whiE* cluster, with conservation of the sequences of ORFs, as well as retention of their size⁶ and position.⁶ Biosynthetic gene clusters associated with spore pigment polyketides appear to be rather common in *Streptomyces*, as Southern blotting experiments revealed *whiE*-homologous clusters in about half of a random collection of *Streptomyces* species.⁷ The KS and CLF subunit sequences of these spore pigment PKS systems are strongly related, and in a phylogenetic analysis, each forms a separate subcluster distinct from the cluster that includes the corresponding antibiotic PKS subunits.^{4,8}

To gain insight into the roles of the *whiE*, *sch*, and *cur* PKSs in spore pigment biosynthesis in *Streptomyces*, we developed a host-vector system that consists of the *S. coelicolor* strain YU105,⁹ from which the *act*-PKS and *whiE*-PKS gene clusters have been deleted, and derivatives of the expression plasmids pRM5 and pSEK4.¹⁰ Here we report the isolation and structure elucidation of nine novel polyketides isolated from recombinants expressing groups of spore pigment PKS genes with and without the *act* KR. Although the natural spore pigment is probably derived from a dodecaketide produced by the *whiE* PKS, analysis of the recombinant containing the *whiE* minimal PKS indicated a relaxed chain length control as polyketides were produced of varying lengths. Naphthyl dodecaketides were only produced when the *whiE*-ORFVI cyclase was combined with the *whiE* minimal PKS, indicating that the cyclase is not only responsible for the cyclization and aromatization of the first two rings but must also coordinate with the minimal PKS to influence chain length control.

(7) Blanco, G.; Brian, P.; Pereda, A.; Méndez, C.; Salas, J. A.; Chater, K. F. *Gene* **1993**, *130*, 107–116.

(8) Seow, K.-h.; Meurer, G.; Gerlitz, M.; Wendt-Pienkowski, E.; Hutchinson, C. R.; Davies, J. J. *Bacteriol.* **1997**, *179*, 7360–7368.

(9) Yu, T.-W.; Hopwood, D. A. *Microbiology* **1995**, *141*, 2779–1791.

(10) McDaniel, R.; Ebert-Khosla, S.; Hopwood, D. A.; Khosla, C. *Science* **1993**, *262*, 1546–1550.

(11) Fu, H.; Ebert-Khosla, S.; Hopwood, D. A.; Khosla, C. *J. Am. Chem. Soc.* **1994**, *116*, 4166–4170.

Table 1. Plasmid Constructions and Resulting Polyketide Products

plasmid	genes	major products
pIJ4293 ^a	<i>whiE</i> -ORFIII, -ORFIV, -ORFV	1, 2, 3, 4
pIJ4294 ^b	<i>whiE</i> -ORFIII, -ORFIV, -ORFV, <i>actIII</i>	5, 6, 7, 8
pIJ4295 ^a	<i>whiE</i> -ORFIII, -ORFIV, -ORFV, -ORFVI	9, 10
pIJ4296 ^a	<i>whiE</i> -ORFIII, -ORFIV, -ORFV, -ORFVI, -ORFVII	9, 10
pIJ4297 ^a	<i>whiE</i> -ORFII, -ORFIII, -ORFIV, -ORFV	1, 2, 3, 4
pIJ4298 ^a	<i>whiE</i> -ORFII, -ORFIII, -ORFIV, -ORFV, -ORFVI	9, 10
pIJ4300 ^a	<i>whiE</i> -ORFII, -ORFIII, -ORFIV, -ORFV, -ORFVI, -ORFVII	not identified
pIJ4301 ^a	<i>sch1</i> , <i>sch2</i> , <i>sch3</i>	1, 2, 3, 4
pIJ4302 ^b	<i>sch1</i> , <i>sch2</i> , <i>sch3</i> , <i>actIII</i>	5, 6, 7, 8
pIJ4303 ^a	<i>curA</i> , <i>curB</i> , <i>curC</i>	1, 2, 3, 4
pIJ4304 ^b	<i>curA</i> , <i>curB</i> , <i>curC</i> , <i>actIII</i>	5, 6, 7, 8
pIJ4305 ^a	<i>curA</i> , <i>curB</i> , <i>curC</i> , <i>curF</i> , <i>curG</i>	9, 10

^a pSEK4 derivative. ^b pRM5 derivative.

Results

A series of 12 plasmids containing spore pigment PKS genes from the *whiE*, *sch* and *cur* clusters were made by inserting the gene sets between the *PacI* and *EcoRI* sites of pRM5 or pSEK4,¹⁰ displacing the *act* genes *actI*-ORF1-3 (encoding the three minimal PKS subunits), *actVII* (ARO), and *actIV* (CYC) (Table 1). The three plasmids derived from pRM5 also contained the *actIII* gene, which encodes the *act* KR that catalyzes ketoreduction at the C9 position of the nascent polyketide backbone during actinorhodin biosynthesis.^{10,11} These plasmids were introduced via transformation into the host *S. coelicolor* YU105 from which the natural chromosomal copies of the *act* and *whiE* gene clusters have been deleted.⁹ All of the recombinants synthesized pigmented polyketides. The known polyketide oracetophenone¹² and nine novel aromatic polyketides were isolated from the apolar pigments in these recombinants and characterized by detailed NMR analysis. This strategy was used to deduce the role(s) of the corresponding spore pigment PKS subunits.

Expression and Analysis of the *whiE* Minimal PKS.

Streptomyces coelicolor YU105/pIJ4293 contains the genes encoding the *whiE* minimal PKS (ORFs III–V) (Table 1). HPLC and NMR analyses of extracts from this strain indicated that approximately a dozen polyketides were produced in roughly comparable amounts (2–10 mg/L), in sharp contrast to the results of expressing other type II minimal PKS gene sets, in which only one or a small number of predominant recombinant polyketides were reported.^{11,13–15} Four structurally related polyketides, TW93a–d (1–4, Scheme 1), were purified from this mixture by successive reversed-phase flash chromatography and reversed-phase HPLC and their structures elucidated by NMR.

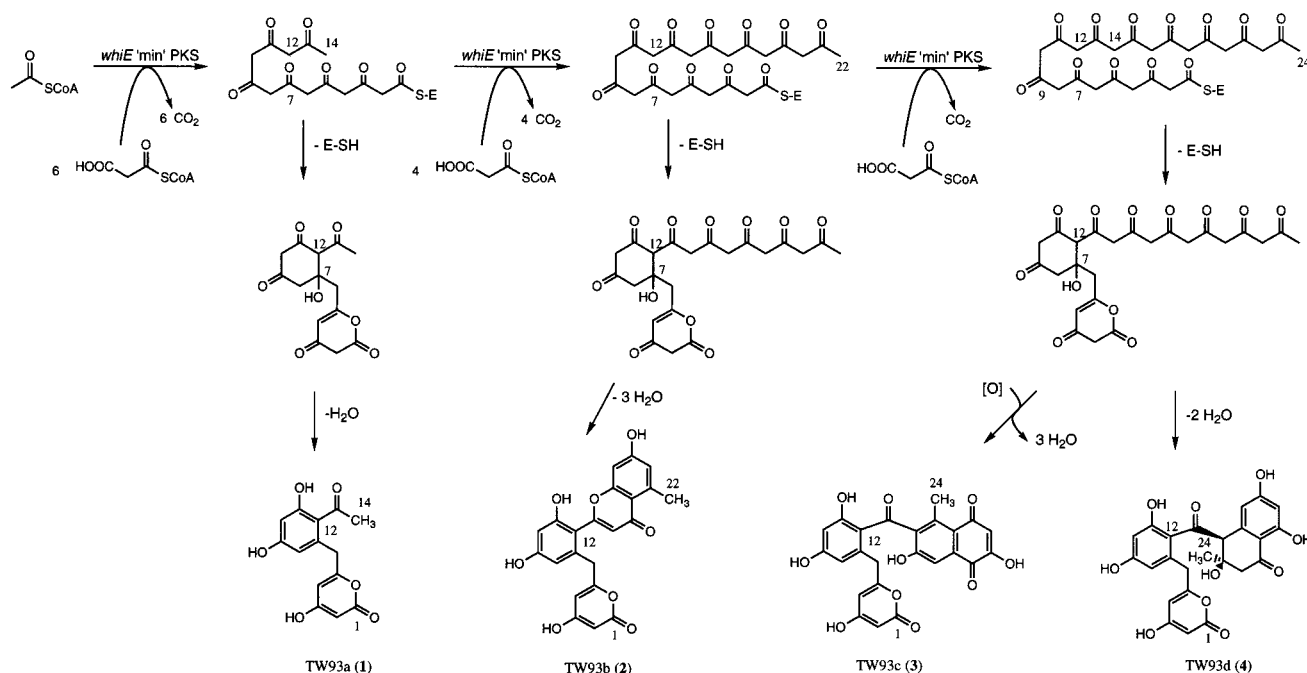
The heptaketide TW93a (1) (4 mg/L) was the shortest of the polyketides and had the formula C₁₄H₁₂O₆ on the basis of high-resolution fast atom bombardment mass spectrometry (HR-FABMS). Analysis of the proton and carbon NMR spectra, with the aid of HMBC (heteronuclear multiple bond correlation) data, clearly indicated that 1 contained pyrone and *o,p*-dihydroxyacetophenone residues (Table 2). Strong IR absorptions at 3412, 1684, and 1676 cm⁻¹ supported the presence of

(12) Hoesch, K. *Chem. Ber.* **1915**, *48*, 1122–1133.

(13) McDaniel, R.; Ebert-Khosla, S.; Fu, H.; Hopwood, D. A.; Khosla, C. *Proc. Natl. Acad. Sci. U.S.A.* **1994**, *91*, 11542–11546.

(14) Fu, H.; Hopwood, D. A.; Khosla, C. *Chem. Biol.* **1994**, *1*, 205–210.

(15) Kramer, P. J.; Zawada, R. J. X.; McDaniel, R.; Hutchinson, C. R.; Hopwood, D. A.; Khosla, C. *J. Am. Chem. Soc.* **1997**, *119*, 635–639.

Scheme 1. Structures and Proposed Biosynthesis of the *whiE*, *sch*, and *cur* Minimal PKS Polyketides TW93a–d (1–4)^a**Table 2.** Proton and Carbon NMR Data for TW93a–d (1–4)^a

no. ^b	TW93a (1)		TW93b (2)		TW93c (3)		TW93d (4)	
	¹³ C	¹ H ^{c,d}	¹³ C	¹ H ^{c,e}	¹³ C	¹ H ^{c,f}	¹³ C	¹ H ^{c,g}
1	164.2		164.1		163.4		163.9	
2	87.7	5.01 (s)	87.9	5.11 (d, <i>J</i> = 1.7)	88.2	5.08 (d, <i>J</i> = 1.8)	88.2	5.17 (d, <i>J</i> = 1.8)
3	172.0		171.4		170.4		170.5	
4	101.4	5.64 (s)	100.2	5.62 (d, <i>J</i> = 1.7)	100.0	5.56 (d, <i>J</i> = 1.8)	100.4	5.69 (d, <i>J</i> = 1.8)
5	164.3		165.2		164.9		166.0	
6	36.4	3.63 (s, 2H)	37.3	4.39 (s, 2H)	37.7	3.78 (s, 2H)	37.0	3.52 (d, <i>J</i> = 16.3) 3.63 (d, <i>J</i> = 16.3)
7	136.0		137.9		139.2		137.3	
8	109.4	6.15 (s)	117.6	6.75 (d, <i>J</i> = 2.0)	112.4	6.26 (d, <i>J</i> = 2.2)	109.7	6.15 (d, <i>J</i> = 2.3)
9	159.5		161.3		162.7		159.9	
10	101.5	6.28 (s)	102.2	6.78 (d, <i>J</i> = 2.0)	102.0	6.22 (d, <i>J</i> = 2.2)	101.6	6.34 (d, <i>J</i> = 2.0)
11	157.8		159.6		163.5		157.8	
12	120.2		113.9		116.3		121.6	
13	202.9		161.0		197.5		203.6	
14	32.2	2.39 (s, 3H)	114.3	6.04 (s)	137.9		60.9	4.94 (s)
15			177.8		156.4		144.8	
16			111.3		111.6	7.35 (s)	109.0	6.56 (d, <i>J</i> = 2.2)
17			156.9		133.3		164.5 ^h	
18			100.5	6.25 (d, <i>J</i> = 1.7)	181.5		101.0	6.14 (d, <i>J</i> = 2.1)
19			159.5		157.6		164.6 ^h	
20			108.6	6.19 (d, <i>J</i> = 1.7)	113.0	5.94 (s)	109.8	
21			138.9		186.4		202.1	
22			19.9	2.12 (s, 3H)	121.6		48.1	H _R 2.44 (d, <i>J</i> = 17.5) H _S 2.97 (d, <i>J</i> = 17.5)
23					138.7		72.3	5.34 (s, OH)
24					18.5	2.29 (s, 3H)	29.3	1.16 (s, 3H)

^a Spectra were obtained at 300 and 500 MHz for proton and 75 and 125 MHz for carbon and were recorded in DMSO-*d*₆. Chemical shifts are reported in δ (ppm). ^b Carbons are labeled according to their number in the polyketide backbone (Figure 3). ^c Coupling constants are presented in hertz. Unless otherwise indicated, all proton signals integrate to 1H. ^d Phenolic proton signals at δ 9.8 and 10.1. ^e Phenolic proton signals at δ 9.6–9.8 (3H), 10.8. ^f Phenolic proton signals at δ 10.5, 10.9, 11.2–11.4 (3H). ^g Phenolic proton signals at δ 9.9, 10.4, 10.7, 11.5, 11.9. ^h Interchangeable.

hydroxyl, aryl ketone, and pyrone functionalities, respectively. A methylene group (C6: δ_C 36.4, δ_H 3.63) was deduced to connect these two moieties based on HMBC correlations (C6 \rightarrow H4, H8; H6 \rightarrow C4, C5, C7, C8, C12) (Table 3).

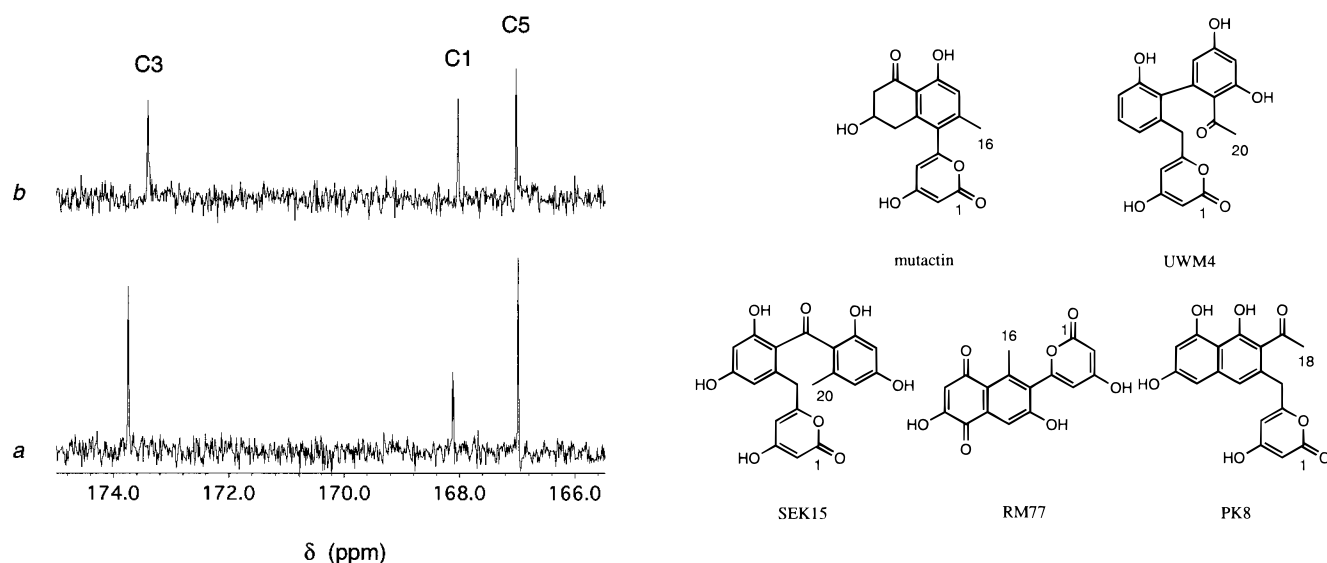
To distinguish between the two possible pyrone desmotropes (2-hydroxy-4-pyrone versus 4-hydroxy-2-pyrone), consecutive ¹³C NMR experiments on equimolar amounts of **1** were performed in CD₃OD and CD₃OH (Figure 2). As expected, an

α -isotope shift¹⁶ of 0.5 ppm was measured at the exchangeable C2 of the pyrone. Additional isotope shifts of 0.4 and 0.1 ppm were observed for C3 and C1, respectively, indicating that C3 experienced two additive β -isotope shifts of approximately 0.1–0.3 ppm each (to H2 and to C3-OH), whereas C1 only

(16) Deuterium substitution typically causes upfield shifts of the carbon atoms α (0.3–0.6 ppm) and β (0.1–0.3 ppm) to the deuterium atom. Hansen, P. E. *Annu. Rep. NMR Spectrosc.* **1983**, *15*, 105–234.

Table 3. Long-Range ^{13}C – ^1H HMBC Correlation Data for **1**–**4**

carbon	1	2	3	4
1	H2	H2	H2	H2
2	H4	H4	H4	H4
3	H2	H2, H4	H2, H4	H2
4	H2, H6	H2, H6	H2, H6	H2, H6a, H6b
5	H4, H6	H4, H6	H4, H6	H4, H6a, H6b
6	H4, H8	H4, H8	H8	H8
7	H6	H6	H6	H6a, H6b
8	H6, H10	H6, H10	H6, H10	H6a, H6b, H10
9	H8, H10	H8, H10	H8, H10	H8, H10
10	H8	H8	H8	H8
11	H10	H10	H10	H10
12	H6, H8, H10, H14	H6, H8, H10, H14	H6, H8, H10	H6a, H6b, H8, H10
13	H14	H14	H16	H14
14			H16, H24	H16, H22 _R , H24
15			H16	H14
16		H14, H18, H20, H22		H14
17		H18	H16	H18
18		H20	H16, H20	H16
19		H18, H20	H20	H18
20		H18, H22		H14, H16, H18, H22 _R
21		H22	H20	H22 _R , H22 _S
22		H20	H16, H20, H24	H14, H24
23			H20, H24	H14, H22 _R , H22 _S , H24
24				H14, H22 _R , H22 _S

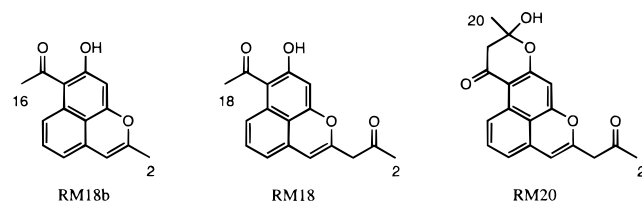
**Figure 2.** Partial ^{13}C NMR spectra of TW93a (**1**) in CD_3OH (a) and CD_3OD (b) at 125 MHz.

experienced one (to H2). The C9 and C11 phenol carbons in the hydroquinone unit experienced β -isotope shifts of approximately 0.2 ppm as well.¹⁷ Therefore, the pyrone enol oxygen must be present at C3 (δ 172.0 in $\text{DMSO}-d_6$), arguing that the pyrone unit in **1** is present as the α -pyrone or γ -lactone and not as the δ -pyrone. Previous reports of structurally related polyketides which contain the identical pyrone unit, such as in mutactin¹⁸ (Figure 3) and several in the RM and SEK series,⁴ are reported as δ -pyrones and should instead be α -pyrones. A similar conclusion was recently obtained for the pyrone unit in the decaketide UWM4 (Figure 3).¹⁹ Single-crystal X-ray crystallography of the UWM4 tetra-*O*-methyl analogue clearly

(17) For ordinary phenols, β -isotope shifts are between 0.12 and 0.15 ppm and γ -isotope shifts are between 0.05 and 0.11 ppm. Newmark, R. A.; Hill, J. R. *Org. Magn. Reson.* **1980**, *13*, 39–44.

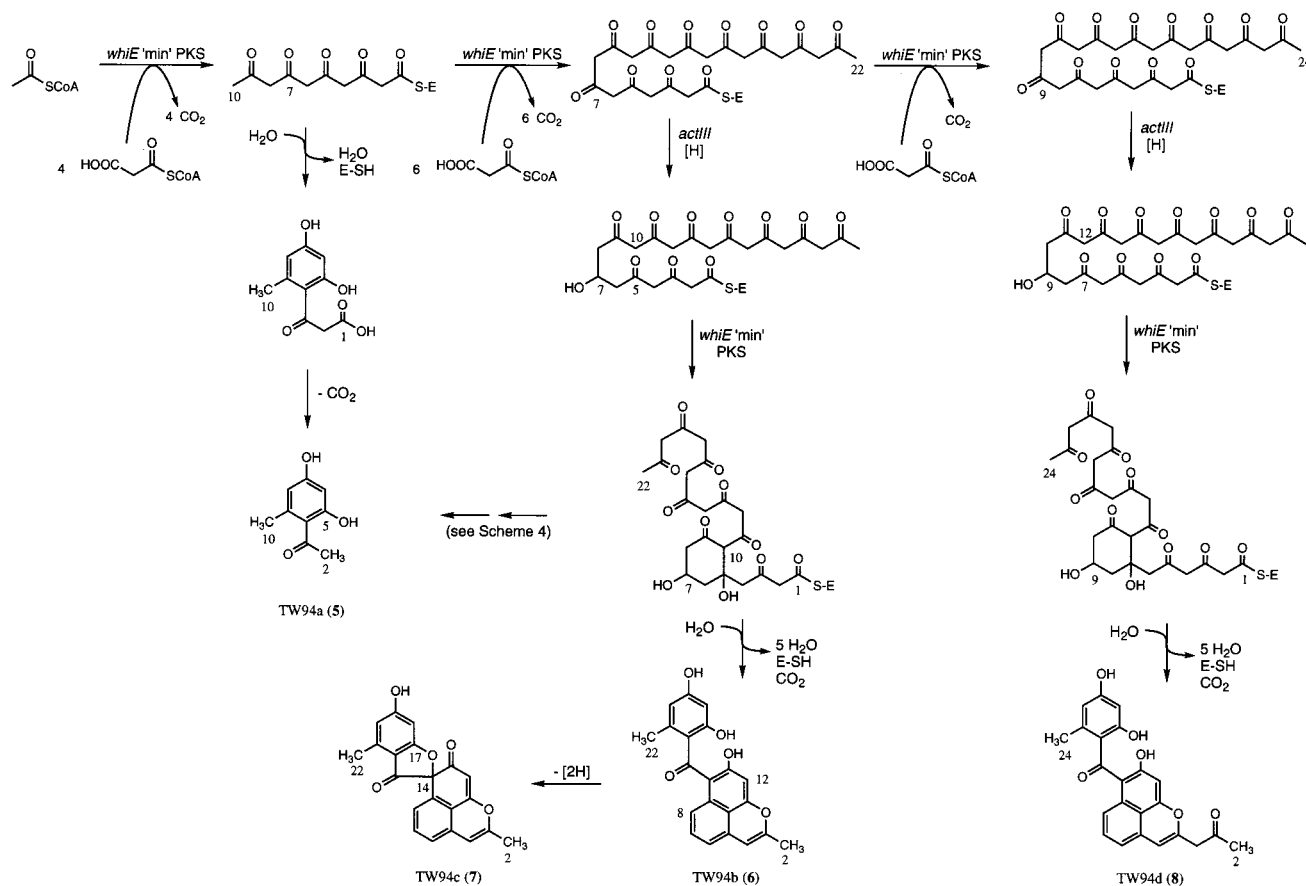
(18) Zhang, H.-l.; He, X.-g.; Adefarati, A.; Gallucci, J.; Cole, S. P.; Beale, J. M.; Keller, P. J.; Chang, C.-j.; Floss, H. G. *J. Org. Chem.* **1990**, *55*, 1682–1684.

(19) Meurer, G.; Gerlitz, M.; Wendt-Pienkowski, E.; Vining, L. C.; Rohr, J.; Hutchinson, C. R. *Chem. Biol.* **1997**, *4*, 433–443.

**Figure 3.** Structures of related recombinant polyketides: mutactin,¹⁸ UWM4 (minimal *tcm* PKS + *dpsE* + *dpsF*),¹⁹ SEK15 (minimal *tcm* PKS + *actVII* and *actIV*),^{11,13} RM77 (minimal *act* PKS + *tcmN*),²⁰ PK8 (minimal *fren* PKS + *tcmN* ± *tcmJ*),¹⁵ RM18 and RM18b (minimal *fren* PKS + *actIII*),²¹ and RM20 (minimal *tcm* PKS + *actIII*).¹⁰

showed that the 3-methoxy and not the 1-methoxy isomer was formed upon methylation.

The C7/C12 cyclization and the 4-hydroxy-2-pyrone in **1** were found to be common structural features in the three larger polyketides (**2**–**4**) isolated from *S. coelicolor* YU105/pIJ4293. These features are also present in the decaketide SEK15 (Figure 3) from *S. coelicolor* CH999/pSEK15.¹¹ Compounds **1**–**4**, as well as SEK15, all differ from each other in the group attached at C12.

Scheme 2. Structures and Proposed Biosynthesis of the *whiE*, *sch*, and *cur* Minimal PKS and *ActIII* Polyketides TW94a–d (5–8)^a

^a TW94c is optically active, but of unknown absolute configuration.

TW93b (**2**) was an undecaketide with a molecular formula of C₂₂H₁₆O₈ based on HRFABMS and was isolated in the lowest yield (3 mg/L) among **1**–**4**. Inspection of the NMR spectral data (proton, carbon, DEPT, HMBC) indicated that **2** had the same structure as **1** from carbons 1 through 12. Moreover, a 10-carbon fragment composed of a 7-hydroxy-5-methylchromone moiety was attached to C12 (Table 2). Three key HMBC correlations between the isolated methine proton at δ 6.04 (H14) and C12, C13, and C16 indicated that the chromone unit is attached at C12 via C13 in a flavone-type arrangement (Table 3). The presence of the chromone functionality at C12 was also supported by the downfield shift of the proton signals at δ 4.39 (H6) and δ 6.75 (H8).

The two dodecaketides TW93c (**3**) and TW93d (**4**) were structurally identical to **1** from carbons 1 through 13 but differed in the cyclization pattern for the remaining 11-carbon fragment (C14–C24). TW93c, the major polyketide isolated from *S. coelicolor* YU105/pIJ4293 at 10 mg/L, had the molecular formula C₂₄H₁₆O₁₀ on the basis of HRFABMS. The NMR spectral data (proton, carbon, DEPT, HMQC, HMBC) indicated that, in addition to 4-hydroxy-2-pyrone and *o,p*-dihydroxyphenyl ketone residues, **3** contained a tetrasubstituted 1,4-naphthoquinone in which the polyketide chain has cyclized C17/C22 and C14/C23 (Table 2). The quinone, which is structurally identical to that in the octaketide RM77²⁰ (Figure 3) and shares similar chemical shift values with it, was elucidated from HMBC correlation data and connected to the ketone carbonyl C13 at C14 via a four-bond correlation to H16 (Table 3).

TW93d (**4**) was obtained as a yellow powder (5 mg/L) and had the molecular composition C₂₄H₂₀O₁₀ as established by HRFABMS. The formula showed that **4** had 2 degrees of unsaturation less than **3**. The presence of the same C1–C13 unit as in **1** was readily assigned by NMR spectral analysis (proton, carbon, DEPT, HMQC, HMBC) and supported by IR spectroscopy. The H6 AB quartet (δ 3.52 and 3.63) indicated that **4** possessed chirality in the 11-carbon unit attached to the ketone carbonyl C13 (Table 2). A second 1,2-disubstituted 3,5-dihydroxybenzene unit was evident by NMR analysis. In addition, the proton NMR spectrum included signals for an isolated methine (H14), a nonequivalent methylene (H22), and a methyl group (H24); a second ketone carbonyl at δ 202.1 was evident by carbon NMR. The quaternary carbon signal at δ 72.3 and the D₂O-exchangeable proton signal at δ 5.34 suggested the presence of a tertiary alcohol on C23. Together with these data, HMBC correlations (Table 3) allowed us to deduce the presence of the 11-carbon α -tetralone unit and its attachment to the dihydroxyphenyl ketone moiety (C13 \rightarrow H14).

The relative stereochemistry of **4** was established by 1D difference NOE experiments. Irradiation of the H24 methyl hydrogens (δ 1.16) resulted in enhancement of the H14 and H22_R (δ 2.44) signals, strongly suggesting that these protons are syn to the methyl group. The other H22_S methylene signal at δ 2.97 was also enhanced, but only weakly in comparison to the H22_R signal. Enhancement of the C23 hydroxyl proton at δ 5.34 was observed upon irradiation of H22_S, further indicating that the hydroxyl group and H22_S proton are arranged in a syn relationship. Notably, **4** did not give a CD signal, suggesting that it exists as the racemate. This finding implies that the ring

Table 4. Proton and Carbon NMR Data for TW94a–d (**5–8**)^a

TW94a (5)			TW94b (6)			TW94c (7)		TW94d (8)		
no. ^b	¹³ C	¹ H ^{c,d}	no. ^b	¹³ C	¹ H ^{c,e}	¹³ C	¹ H ^{c,f}	no. ^b	¹³ C	¹ H ^{c,g}
			2	18.7	2.10 (s, 3H)	18.9	2.27 (s, 3H)	2	29.6	2.21 (s, 3H)
			3	152.3		153.7		3	203.7	
			4	104.0	6.12 (s)	103.5	6.49 (s)	4	46.9	3.63 (s, 2H)
			5	129.9		131.0		5	149.7	
			6	114.2	6.68 (d, <i>J</i> = 7.0)	125.1	7.40 (d, <i>J</i> = 7.8)	6	106.8	6.19 (s)
			7	130.1	7.13 (dd, <i>J</i> = 8.6, 7.0)	133.4	7.57 (t, <i>J</i> = 7.7)	7	129.3	
			8	119.2	6.99 (d, <i>J</i> = 8.6)	124.2	7.10 (d, <i>J</i> = 7.6)	8	114.7	6.72 (d, <i>J</i> = 7.1)
			9	133.5		135.1		9	130.1	7.15 (dd, <i>J</i> = 8.6, 7.1)
			10	119.1		117.6		10	119.7	7.02 (d, <i>J</i> = 8.6)
			11	159.5		167.2 ⁱ		11	133.4	
			12	98.6	6.44 (s)	98.8	5.68 (s)	12	118.9	
			13	157.0		187.2		13	159.8	
2	32.4	2.41 (s, 3H)	14	113.2		93.0		14	98.7	6.39 (s)
3	203.0		15	199.5		190.3		15	156.7	
4	119.0		16	116.5		106.1		16	113.5	
5	159.2 ^h		17	160.8		176.3		17	199.4	
6	100.3	6.14 (d, <i>J</i> = 2.0)	18	100.7	6.17 (s)	96.0	6.57 (s)	18	116.7	
7	160.2 ^h		19	161.4		167.3 ⁱ		19	160.9	
8	109.8	6.08 (d, <i>J</i> = 2.0)	20	110.1	6.17 (s)	113.8	6.46 (s)	10	100.7	6.15 (s)
9	139.1		21	139.0		142.4		21	161.0	
10	21.0	2.16 (s, 3H)	22	20.2	1.92 (s, 3H)	17.3	2.31 (s, 3H)	22	110.1	6.15 (s)
								23	139.3	
								24	20.3	1.92 (s, 3H)

^a Spectra were obtained at 300 and 500 MHz for proton and 75 and 125 MHz for carbon and were recorded in DMSO-*d*₆. Chemical shifts are reported in δ (ppm). ^b Carbons are labeled according to their number in the polyketide backbone; hence C1 is absent due to its loss as CO₂ during biosynthesis (Scheme 1). ^c Coupling constants are presented in hertz. Unless otherwise indicated, all proton signals integrate to 1H. ^d Phenolic proton signals at δ 9.7 and 10.6. ^e Phenolic proton signals at δ 9.9, 10.9, 12.6. ^f Phenolic proton signal at δ 10.9. ^g Phenolic proton signals at δ 9.9, 11.2, 12.6. ^{h,i} Interchangeable.

closure of the α -tetralone moiety is either not enzymatically controlled or is enzymatically controlled but chemically racemizes via a retro-aldol reaction.

Influence of *actIII* (Ketoreductase) on the *whiE* Minimal PKS. The influence of the *act* KR on the *whiE* minimal PKS chain length specificity and cyclization pattern was examined in the construct YU105/pIJ4294. In this case, four polyketides with odd numbers of carbons predominated in the extract, contrasting with the previous result on the expression of the *whiE* minimal PKS alone which produced a much more complex mixture of products. The known *unreduced* nine-carbon polyketide oracetophenone,¹² designated TW94a (**5**), and three novel *reduced* polyketides TW94b–d (**6–8**) (Scheme 2) were isolated from this recombinant by successive normal-phase flash chromatography and reversed-phase HPLC.

TW94a (**5**) was isolated in the lowest yield (1.5 mg/L) among the four major polyketides produced by YU105/pIJ4294. Because **5** had not been fully characterized in the literature, to the best of our knowledge, and was a common structural component in **6** and **8**, verification and assignment of its structure was necessary. Spectral features for **5** (C₉H₁₀O₃ based on HRFABMS) were readily assigned by proton and carbon NMR analysis (Table 4) and were supported by strong IR absorptions at 3426 and 1686 cm⁻¹ for hydroxyl and benzylic ketone functionalities, respectively. Assignment of the phenyl proton signal at δ 6.08 (H8) was established through a difference NOE experiment in which irradiation of the benzylic methyl protons on C9 resulted in the enhancement of this signal.

TW94b (**6**) was obtained as a yellow solid (4.5 mg/L) and had the molecular formula C₂₁H₁₆O₅ on the basis of HRFABMS. Spectral features for the 2,4-dihydroxy-6-methylphenyl ketone residue, analogous to that in **5**, were readily assigned (Table 4). The remaining 13-carbon tricyclic aromatic system in **6** was identified through spectral similarities with RM18b²¹ (Figure

Table 5. Long-Range ¹H–¹³C Correlation Data for **6** and **7**

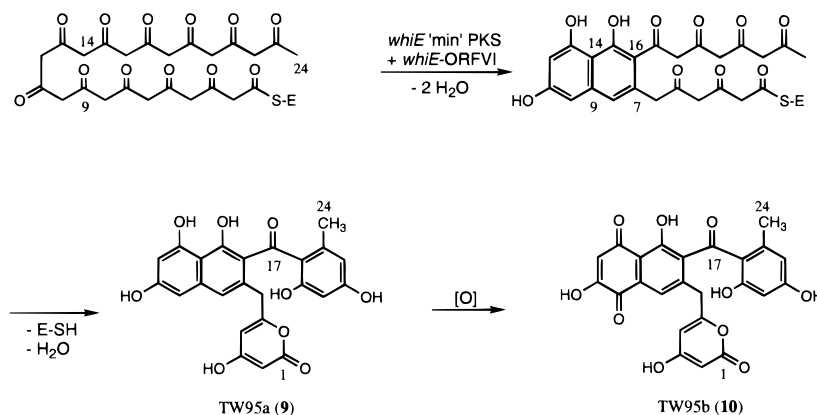
proton	TW94b (6) ^a	TW94b (7) ^b
2	C3, C4	C3, C4
4	C2, C5, C6, C10	C2, C3, C6, C10
6	C4, C8, C10	C4, C5, C7, C8, C10
7	C5, C9	C5, C6, C9
8	C6, C9, C10, C14	C6, C10, C14
12	C10, C11, C13, C14	C10, C11, C13, C14
18	C16, C17, C19, C20	C16, C17, C19, C20
20	C16, C18, C19, C21, C22	C16, C18, C22
22	C16, C20, C21	C16, C20, C21

^a FLOCK correlation data. ^b HMBC correlation data.

3). NMR experiments, notably 1D difference NOE and 2D HETCOR and FLOCK heterocorrelation measurements (Table 5), confirmed the structure and allowed us to assign all of the carbons and their respective protons.

A second 21-carbon metabolite, TW94c (**7**) (2.5 mg/L), analyzed for C₂₁H₁₄O₅ by HRFABMS, had 1 degree of unsaturation more than **6**. HMBC data indicated that **7** and **6** had the same carbon skeleton (Table 5). Two ketone carbonyls and one phenolic group were detected by carbon and proton NMR (Table 4), respectively, suggesting that the two remaining oxygens in **7** were present as ethers. The presence of the isochromene moiety was supported by spectral analysis; however, the NMR signals were shifted appreciably downfield in **7** relative to those in **6**, indicating that the ring system was less electron-rich. The isolated olefin proton signal at δ 5.68 (H12) was significantly shifted upfield compared with the same signal (δ 6.44) for **6**, as H12 was on the relatively electron-rich α -carbon of the α,β -unsaturated ketone. HMBC correlations from the quaternary carbon resonating at δ 93.0 (C14) to H8 and H12 completed the structure of the tricyclic ring system. Spectral features indicating the presence of a 2,4-dioxy-6-methylphenyl ketone functionality in **7** could be easily seen. The differences in chemical shifts for this unit compared with those in **6** were rationalized by the presence of a fused furanone

(21) McDaniel, R.; Ebert-Khosla, S.; Hopwood, D. A.; Khosla, C. *J. Am. Chem. Soc.* **1993**, *115*, 11671–11675.

Scheme 3. Structures and Proposed Biosynthesis of the *whiE* and *cur* Minimal PKS plus *whiE*-ORFVI Polyketides TW95a (**9**) and TW95b (**10**)

system, which accounted for the extra degree of unsaturation. The ether connectivity between C14 and C17 of the furanone residue was supported by the dramatic downfield shift of the C17 signal (δ 176.3), which was in agreement with the increased chemical shift for a cyclopentenone β -carbon.²²

Optical rotation and CD analyses indicated that **7** was optically active. Its absolute configuration, however, could not be assigned by the CD exciton chirality method because of overlapping split CD Cotton effects. TW94b is probably converted enzymatically in an unprecedented post-PKS dehydrogenation by a resident *S. coelicolor* enzyme into the optically active (at C14) furanone analogue TW94c (Scheme 2). TW94b and TW94c were isolated in approximately a 2:1 ratio.

The major metabolite (5.5 mg/L) isolated from *S. coelicolor* YU105/pIJ4294 was the 23-carbon compound TW94d (**8**), which had a molecular formula of $C_{23}H_{18}O_6$ on the basis of HRFABMS. Inspection of the NMR spectral data (Table 4) and structural comparison with RM18²¹ (Figure 3) indicated that **8** was the acetyl analogue of **6**. These TW94 tricyclic polyketides structurally resemble polyketides derived from other minimal PKS + *actIII* constructs, such as RM18 and RM18b (*fren* minimal PKS + *actIII*)²¹ and RM20 (*tcm* minimal PKS + *actIII*)¹⁰ (Figure 3). In each case they contain a related tricyclic ring system differing mainly in the substitution pattern, and all of them have lost C1 by decarboxylation. Surprisingly, the furanone derivative of TW94d was not identified in the extract mixture. This finding seems to further imply that TW94c is indeed an enzymatic product.

Properties of the *whiE* Cyclases (*whiE*-ORFs II, VI, and VII). The deduced gene products of *whiE*-ORFs II, VI, and VII strongly resemble cyclase/aromatase enzymes from the tetracenomycin biosynthetic gene cluster (Figure 1); these are *tcmJ*, the N-terminal half of *tcmN*, and *tcmI*, respectively.^{15,20,23–25} To analyze the properties of the presumed *whiE* cyclases, plasmids containing the minimal *whiE* PKS were constructed with various combinations of the *whiE* cyclase genes (Table 1). Earlier observations on spore pigmentation induced by plasmids carrying incomplete sets of the *whiE* genes indicated that the order of action of the cyclases in the biosynthesis of the spore pigment was VI \rightarrow II \rightarrow VII.⁹

(22) Kalinowski, H.-O.; Berger, S.; Braun, S. *¹³C NMR-Spektroskopie*; Georg Thieme Verlag: Stuttgart, 1984.

(23) Summers, R. G.; Wendt-Pienkowski, E.; Motamedi, H.; Hutchinson, C. R. *J. Bacteriol.* **1992**, *174*, 1810–1820.

(24) Summers, R. G.; Wendt-Pienkowski, E.; Motamedi, H.; Hutchinson, C. R. *J. Bacteriol.* **1993**, *175*, 7571–7580.

(25) Shen, B.; Summers, R. G.; Wendt-Pienkowski, E.; Hutchinson, C. R. *J. Am. Chem. Soc.* **1995**, *117*, 6811–6821.

Table 6. Proton and Carbon NMR Data for TW95a (**9**) and TW95b (**10**)^a

no. ^b	TW95a (9)		TW95b (10)	
	¹³ C	¹ H ^{c,d}	¹³ C	¹ H ^{c,e}
1	163.8		163.4	
2	88.5	5.19 (d, <i>J</i> = 1.9)	88.7	5.18 (d, <i>J</i> = 2.0)
3	172.3		170.1	
4	101.1	5.70 (d, <i>J</i> = 1.8)	101.5	5.75 (d, <i>J</i> = 2.0)
5	164.2		162.6	
6	37.3	3.71 (s, 2H)	36.5	3.75 (s, 2H)
7	131.4		137.7	
8	119.3	7.00 (s)	119.8	7.45 (s)
9	137.8		130.3	
10	101.6	6.60 (d, <i>J</i> = 1.9)	180.7	
11	158.1		162.0 ^f	
12	101.5	6.46 (d, <i>J</i> = 2.0)	109.9	6.04 ^g (s)
13	156.2		190.4	
14	107.8		113.6	
15	154.9		157.0 ^f	
16	120.1		139.4	
17	199.6		195.0	
18	117.2		116.3	
19	162.3		163.1	
20	100.7	6.17 (s)	100.6	6.09 (d, <i>J</i> = 1.9)
21	163.1		162.8	
22	111.1	6.13 (s)	111.5	6.15 (d, <i>J</i> = 1.9)
23	141.9		142.9	
24	21.1	1.90 (s, 3H)	21.9	2.14 (s, 3H)

^a Spectra were obtained at 300 and 500 MHz for proton and 75 and 125 MHz for carbon and were recorded in DMSO-*d*₆. Chemical shifts are reported in δ (ppm). ^b Carbons are labeled according to their number in the polyketide backbone (figure 3). ^c Coupling constants are presented in hertz. Unless otherwise indicated, all proton signals integrate to 1H. ^d Phenolic proton signals at δ 10.0, 10.2, 11.5 (3H), 12.0. ^e Phenolic proton signals at δ 10.3, 11.1, 11.6 (2H), 12.9. ^f Interchangeable. ^g Exchangeable with D₂O.

Two dodecaketides were isolated from extracts of *S. coelicolor* YU105/pIJ4295, which contains the *whiE*-ORFVI aromatase/cyclase along with the *whiE* minimal PKS. Normal-phase flash chromatography yielded the major yellow-pigmented metabolite TW95a (**9**) (Scheme 3) at 50 mg/L. The structurally related orange-pigmented TW95b (**10**) was isolated at 8 mg/L after successive normal-phase flash chromatography, reversed-phase HPLC, and LH-20 gel filtration.

TW95a (**9**) had the molecular formula $C_{24}H_{18}O_9$ on the basis of HRFABMS. Evidence for the 4-hydroxy-2-pyrone functionality as in **1–4** and the 2,4-dihydroxy-6-methylphenyl ketone functionality as in **6** and **7** was obtained by NMR spectral analysis (proton, carbon, DEPT, HETCOR, FLOCK) (Table 6) and supported by IR spectroscopy. The remaining 10-carbon trihydroxy naphthyl moiety was established from ¹H–¹³C long-

Table 7. Long-Range ^1H – ^{13}C Correlation Data for **9** and **10**

proton	9 ^a	10 ^b
2	C1, C3, C4	C1, C3, C4
4	C2, C3, C5	C2, C3, C5, C6
6	C4, C5, C7, C8, C16	C4, C5, C7, C8, C16
8	C6, C9, C10, C14, C16	C6, C10, C13, C14, C16, C17
10	C8, C11, C12, C14	
12	C10, C11, C13, C14	C10, C11, C13, C14
20	C18, C19, C21, C22	C18, C19, C21, C22
22	C18, C20, C21, C24	C18, C20, C24
24	C18, C22, C23	C18, C22, C23

^a FLOCK correlation data. ^b HMBC correlation data.

range FLOCK heterocorrelation data via H8, H10, and H12 (Table 7). Attachment of the α -pyrone unit via the C6 methylene to C7 was evident from difference NOE and FLOCK measurements.

TW95a is structurally related to the *S. coelicolor* CH999/pPK8 nonaketide PK8¹⁵ (Figure 3), differing only in the substitution at C17 where PK8 contains a methyl group. Spectral comparison of the two compounds indicates that the quaternary carbons C7, C9, C14, and C16 in PK8 were probably misassigned. In the case of PK8, the assignment of the carbons was largely based on ^{13}C – ^{13}C coupling constants of similar magnitude derived from a sample of PK8 biosynthesized from [1,2- $^{13}\text{C}_2$]acetate.

The second dodecaketide, TW95b (**10**), was assigned the molecular composition $\text{C}_{24}\text{H}_{16}\text{O}_{10}$ by HRFABMS, which has 1 degree of unsaturation more than **9**. HMBC data showed that **10** and **9** had the same carbon skeleton (Table 7), differing only in the oxidation pattern of the naphthyl unit. Since the UV absorption bands for **10** were red-shifted compared to those for **9** and two additional ketone carbonyl signals were present in the ^{13}C NMR spectrum, **10** probably contained a naphthoquinone residue to account for the additional degree of unsaturation in its molecular formula. The presence of the naphthoquinone moiety in **10** was supported by the downfield shift of the H8 signal, the upfield shift of the D₂O-exchangeable H12 signal, and the absence of a H10 signal. Final assignment of the disubstituted 2,6-dihydroxy-1,4-naphthoquinone residue was made through HMQC and HMBC heterocorrelation measurements.

A third red pigment, which we suspect is a dimer of **10** at C11 through an ether connection, was isolated during LH-20 gel filtration from the HPLC fraction containing **10** at 10 mg/L. Complete structural analysis of this pigment, however, has been hampered, because we have not been able to generate a molecular ion for this compound. The results of NMR analyses, including HMQC and HMBC experiments, of the suspected dimer were nearly identical to those of **10**. The main differences between the two pigments were that H8 and H12 were shifted upfield by 0.18 and 0.57 ppm, respectively, and that C10–C13 were shifted. Upon standing at 4 °C, **10** slowly converted to this metabolite.

Expression of the cyclase gene *whiE*-ORFII with the *whiE* minimal PKS resulted in the same products as detected in *S. coelicolor* YU105/pIJ4293 (including **1**–**4**), confirming that *whiE*-ORFII acts after *whiE*-ORFVI.⁹ Individual expression of either *whiE*-ORFII or *whiE*-ORFVII with the *whiE* minimal PKS containing *whiE*-ORFVI did not change the chemistry of pigmentation in these strains; **9** and **10** were generated in levels comparable to those produced when these genes were missing. Only when *whiE*-ORFs II and VII were expressed together with the *whiE* minimal PKS and *whiE*-ORFVI in *S. coelicolor* YU105/pIJ4300 were **9** and **10** absent and new pigments

produced instead. Red and blue pigments were isolated, albeit impure and in very low yields. Work is currently underway to isolate and identify these metabolites, which should more closely resemble in structure the true wild-type *whiE* spore pigment.

Analysis of the *sch* and *cur* Gene Clusters. The genes in the *sch*⁵ and *cur*⁶ clusters are highly homologous in sequence to the *whiE* genes, with conservation of the ORFs, as well as retention of their the size and position (Figure 1). Expression of the *sch* and *cur* minimal PKS genes in YU105/pIJ4301 and YU105/pIJ4303, respectively, resulted in the production of **1**–**4** in amounts similar to those isolated from the strain containing the *whiE* minimal PKS alone (Table 1). Furthermore, expression of the *actIII* ketoreductase gene with the *sch* and *cur* minimal PKS genes and expression of the *curF* and *curG* (the homologues of *whiE*-ORFs VI and VII) genes with the *cur* minimal PKS gave **5**–**8**, **9**, and **10** in comparable yields to those isolated from similar constructions with the *whiE* minimal PKS (Table 1). These findings support the idea that these three highly homologous gene clusters encode enzymes needed for the biosynthesis of structurally related spore pigments and suggest that the occurrence of dodecaketide spore pigments may be commonplace in *Streptomyces*.

Discussion

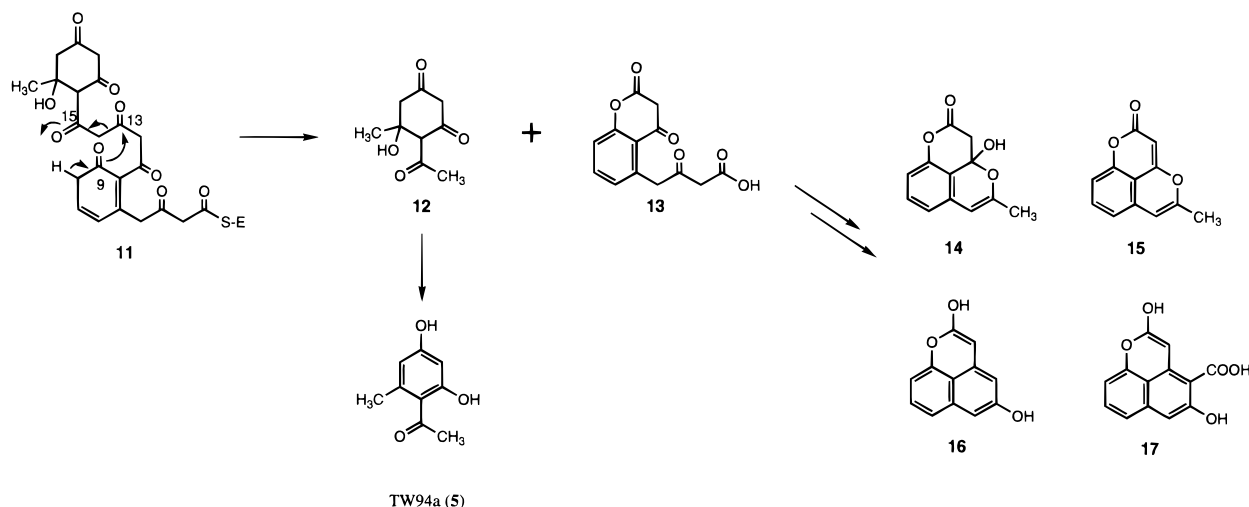
Four sets of novel polyketides were produced by expressing various components of the *whiE*, *sch*, and *cur* spore pigment PKS gene clusters in the *S. coelicolor* YU105 host. Structural analysis of these engineered metabolites allowed us to dissect the function(s) of the individual components of spore pigment PKSs.

The *whiE* minimal PKS construct YU105/pIJ4293, as well as the analogous *sch* and *cur* constructs, yielded a large family of approximately a dozen polyketides in roughly equal amounts from which TW93a–d were isolated and characterized. TW93a–d differ only in the unit attached at C12. The first cyclization event involves an aldol condensation between C7 and C12 and is probably influenced by the minimal PKS (Scheme 1). Aromatization of the first ring and formation of the α -pyrone and the C13–C22/C24 units, however, are most likely spontaneous chemical reactions. The dodecaketides TW93c and TW93d were the most abundant and differed only in the cyclization pattern of the C13–C24 bicyclic moiety. These residues are probably formed without enzymatic control; this is most apparent in TW93d in which the α -tetralone moiety is racemic. In the unlikely event that the α -tetralone unit is alternatively formed enzymatically, it then may chemically racemize through a retro-aldol reaction.²⁶

This large structural variety of polyketides was not observed in the other *whiE* constructs which contained additional genes. This was very apparent for pIJ4295, which contained the *whiE*-ORFVI cyclase in addition to the *whiE* minimal PKS genes (Scheme 3). The dodecaketide TW95a and its oxygenated analogue TW95b were essentially the only polyketides isolated from this recombinant and were produced in the greatest overall yield (up to 60 mg/L) in comparison to those polyketides produced by the other constructs.

Addition of the *whiE*-ORFII gene product to the minimal PKS proteins, with or without the *whiE*-ORFVI cyclase, had no effect on the resulting metabolites. Similarly, *whiE*-ORFVII had no effect on polyketide production. Similar results were obtained with the homologous *tcmJ* gene in the *tcm*²⁵ and *fren*¹⁵ systems. Only when the complete set of three *whiE* cyclases was

(26) Mutactin¹⁸ (Figure 3), which is racemic at C9, is thought to be formed in such a manner.

Scheme 4. Hypothetical Fragmentation of the *Reduced* Undecaketide **11**, an Intermediate of **6** Biosynthesis, To Yield TW94a (**5**) and the Chromones **14–17**

expressed together with the *whiE* minimal PKS in the recombinant YU105/pIJ4300 was a further set of polyketide pigments generated. It seems that *whiE*-ORFs II and VII act in concert with the remainder of the *whiE* PKS subunits to facilitate construction of the nearly complete spore pigment polyketide. We have only been able to isolate small amounts of two highly aromatic polyketides from the recombinant containing all three cyclases (*whiE*-ORFs II, VI, and VII) but require more sample for a complete structural analysis.

A mixture of decarboxylated polyketides (TW94b–d) derived from undecaketides and dodecaketides was produced when the *whiE* minimal PKS was expressed with the *act* KR (Scheme 2). TW94b–d are all *reduced* polyketides, indicating that the *act* KR is able to operate on much longer chains than it normally encounters. In contrast, TW94a (**5**), which was also isolated in relatively high yield, is an *unreduced* compound. As implied in Scheme 2, **5** may be a derailment product derived from an unreduced pentaketide.²⁷ However, if this were the case, additional short chain polyketides might have been formed. Yet, **5–8** were clearly the major polyketides produced in YU105/pIJ4294.

Therefore, we hypothesize instead that **5**, which is a common structural component in **6–8**, is derived by a nonenzymatic fragmentation of a structurally related intermediate in the biosynthesis of **6** and/or **8**. Attack of the C9 oxygen on the C13 carbonyl carbon of the undecaketide **11** would result in cleavage of the C14–C15 bond, leading to two byproducts, the pre-aromatized TW94a metabolite **12** and the 2,4-chromandione **13** (Scheme 4). Dehydration and tautomerization of **12** would thus yield **5**, whereas several metabolites (**14–17**) are potentially derived from **13**. In an analogous fashion, **5** and a different set of tricyclic metabolites are envisaged as cleavage products from a homologous dodecaketide intermediate in the biosynthesis of **8**. In both cases though, **5** is a common fragmentation product which we isolate in a relatively high yield. We are currently analyzing the minor components in the extracts from this recombinant for the proposed tricyclic products to corroborate this hypothesis.

The new results described here are interesting in several respects. One concerns the control of carbon chain length. There is a prior example of relaxed chain length control among type

(27) Biomimetic studies with linear β -polyketones have shown that these undergo aldol condensations to form related aromatic phenolic compounds. Harris, T. M.; Harris, C. M. *Pure Appl. Chem.* **1986**, *58*, 283–294.

II PKSs: the *fren* minimal PKS is able to assemble both C16 (octaketide) and C18 (nonaketide) chain lengths when expressed in the *S. coelicolor* heterologous host along with the *act* KR, while alone it produces only C16 compounds, and in the presence of *tcmN*, only C18 chains.²⁸ This relaxed chain length control is applied in the natural host for the *fren* genes, *S. roseofulvus*, which produces both the octaketide antibiotic nanaomycin and the nonaketide frenolicin from the same PKS.^{29,30} Presumably the *fren* analogue of the *act* KR plays a comparable role in nature as the *act* KR does in the recombinant experiments. In the experiments described here with the spore pigment genes, mixtures of undecaketides and dodecaketides were produced by the minimal PKS alone or in the presence of the (unnatural) *act* KR, whereas when the *whiE*-ORFVI cyclase was present, only dodecaketides arose, in high yield. This implies that the *whiE* minimal PKS requires an additional subunit (the cyclase) to stabilize the complex between the long nascent polyketide chain and the minimal PKS to ensure that the chain reaches the full 24 carbons. On this point, the natural spore pigment is predicted to be a C24 compound, rather than C22 or a mixture of C22 and C24 structures.

The additional presence of the heptaketide TW93a (**1**, Scheme 1), as well as the several uncharacterized polyketides from the *whiE* minimal PKS recombinant, presents an interesting scenario in regards to chain length control. Without the stabilizing effect of the *whiE*-ORFVI cyclase, the *whiE* CLF may be possibly very promiscuous, which results in the production of the shortened heptaketide and the other uncharacterized (and shorter?) polyketides. Alternatively, as in the case of TW94a (Scheme 4), TW93a may likewise be a degradation product arising from biosynthetic intermediates of structurally related, longer polyketides.

A second important issue in aromatic polyketide assembly concerns the primary fold of the nascent chain, established by the first aldol condensation occurring in the middle region.

(28) Summarized in ref 4, figure 11.

(29) Bibb, M. J.; Sherman, D. H.; Omura, S.; Hopwood, D. A. *Gene* **1994**, *142*, 31–39.

(30) Recently, four additional genes (a FAB H homolog, a second ACP, an acyl transferase, and an *act5B* homolog) have been sequenced upstream of the *fren* minimal PKS that may specify the use of a butyryl-CoA starter unit instead of acetyl-CoA (GenBank AF058302). This may be the reason for the production of C16 and C18 metabolites in *S. roseofulvus* instead of a relaxed chain length control by the *fren* minimal PKS. C. D. Reeves, personal communication.

Again, there are prior examples where this condensation involves a different pair of carbons in recombinant experiments as in the natural host.⁴ The *tcm* minimal PKS, expressed in *S. coelicolor* in the presence of other (unnatural) PKS subunits of the *act* PKS, generated molecules predominantly or exclusively with a C7/C12 first ring closure,^{10,31} whereas a C9/C14 condensation is exclusively found in the natural host for the *tcm* genes, *S. glaucescens*,²⁵ and was found in a high proportion of the products when the *tcm* minimal PKS was expressed alone in *S. coelicolor*.¹³ The finding of an exclusive C9/C14 first condensation when the *whiE* minimal PKS was expressed together with its normal partner, the *whiE*-ORFVI cyclase (or with its *tcmN* homolog²⁵), suggests this as the natural structural feature of the spore pigment. Expression of the *tcm* minimal PKS with the *whiE*-ORFVI cyclase³² or with its *tcmN* homolog²⁰ in *S. coelicolor* yielded C20 products also having a C9/C14 first condensation, which is consistent with the results presented here.

The generation of post-PKS modified polyketide products by endogenous host-encoded enzymes illustrates a third important issue in engineered polyketides. In the results described here, several modified polyketides were reported. The optically active furanone TW94c is probably formed from TW94b in an unprecedented dehydrogenation reaction by an endogenous *S. coelicolor* dehydrogenase (Scheme 2).³³ Also, if the heptaketide TW93a and the nine-carbon polyketide TW94a are products of hydrolysis, then these too are representative of a similar situation.

Isolation of the same aromatic polyketide products from the recombinants carrying corresponding genes from the *whiE*, *sch*, and *cur* gene clusters suggests that the various spore pigments observed in *Streptomyces* spp. are derived from similar or identical polycyclic aromatic polyketide intermediates and, on the basis of the arguments outlined above, would be C24 molecules with a pentacenequinone structure which is first cyclized C9 to C14. Diversity of structure may, however, be introduced by the presence of different sets of tailoring enzymes encoded by non-PKS genes in the various spore pigment gene clusters. For example, *whiE*-ORFVIII and *sch*-ORFC are homologues of each other and of a dichlorophenol hydroxylase from *Alcaligenes eutrophus*.^{7,9,34} Mutations of *whiE*-ORFVIII result in a change of pigmentation in *S. coelicolor* from the wild-type gray to a greenish color,⁹ whereas mutations in *sch*-ORFC alter the spore color from green to lilac in *S. halstedii*.⁷ Thus the spore pigments may well be decorated by different hydroxylation patterns in various *Streptomyces* species.

Finally, there is an interesting parallel between the developing studies of spore pigment biochemical genetics in *Streptomyces* spp. and in filamentous fungi. As in *Streptomyces* spp., fungal spore pigments are often refractory to direct structural analysis, sometime because the simple polyketide precursors undergo oxidative polymerization to yield high molecular weight materials (melanins) that are tightly bound to the cell walls. However, the orange pigment parasperone A (Figure 4) isolated from a laccase-deficient strain of *Aspergillus parasiticus* is a hydroxy-

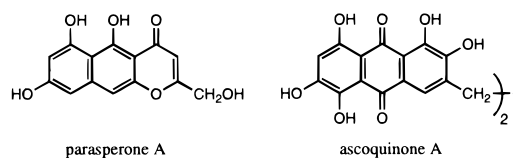


Figure 4. Structures of the fungal spore pigments parasperone A and ascoquinone A.

lated naphtho[2,3-*b*]pyran, which is believed to be a biosynthetic intermediate of the structurally unknown green conidia spore pigment.³⁵ Another spore-related polyketide pigment, ascoquinone A (Figure 4), has been isolated from the ascospores of *A. nidulans*.³⁶ The type I PKS encoded by the *wA* gene of this species may be involved in parasperone A biosynthesis.³⁷

Experimental Section

Spectral Analysis. The ¹H and ¹³C NMR spectra were obtained on IBM AF-300 and Bruker AM-500 spectrometers operating at field strengths of 7.1 and 11.7 T, respectively. ¹H and ¹³C chemical shifts are referenced in DMSO-*d*₆ at 2.50 and 39.5 ppm, respectively. One-bond heteronuclear ¹H-¹³C connectivities were determined by proton-detected HMQC³⁸ or carbon-detected HETCOR experiments. Multiple-bond ¹H-¹³C connectivities were determined by proton-detected HMBC³⁹ or carbon-detected FLOCK⁴⁰ experiments. Homonuclear ¹H NOEs were obtained by difference NOE experiments using a 0.7-s irradiation period. UV and CD spectra were measured in EtOH and CH₃CN, respectively, at 25 °C.

Bacterial Strains and General Techniques for DNA Manipulations. *S. coelicolor* YU105⁹ was used as a host for transformation by all plasmids. The *Escherichia coli* hosts were the strain Epicurian Coli XL1-Blue (Stratagene) for the manipulation of plasmid DNA and the nonmethylating (*dam dcm*) strain SCS110 (Stratagene) to obtain DNA for transformation of *S. coelicolor*. General culture conditions and recombinant DNA techniques for *Streptomyces* spp. and *E. coli* were as described by Hopwood et al.⁴¹ and Sambrook et al.,⁴² respectively.

Construction of Plasmids. pIJ4293 is a derivative of pSEK4¹⁰ in which the *act*-PKS genes were replaced by a 3.2 kb *PacI*-*EcoRI* *whiE*-PKS fragment. *PacI* and *EcoRI* were introduced by cloning the 3.2 kb *Bsp*HI-*NruI* fragment from pIJ4274⁹ into pT1.¹⁰ pIJ4294 is a derivative of pRM5¹⁰ in which the *act*-PKS genes were replaced by a 3.2 kb *PacI*-*EcoRI* *whiE*-PKS fragment. *PacI* and *EcoRI* were introduced by cloning the 3.2 kb *Bsp*HI-*NruI* fragment from pIJ4274 into pT1. pIJ4295 is a derivative of pSEK4 in which the *act*-PKS genes were replaced by a 3.4 kb *PacI*-*EcoRI* *whiE*-PKS fragment. *PacI* and *EcoRI* were introduced by cloning the 3.4 kb *Bsp*HI-*XmnI* fragment from pIJ4274 into pT1. pIJ4296 is a derivative of pSEK4 in which the *act*-PKS genes were replaced by a 3.7 kb *PacI*-*EcoRI* *whiE*-PKS fragment. *PacI* and *EcoRI* were introduced by cloning the 3.7 kb *Bsp*HI-*SphI* fragment from pIJ4274 into pT1. pIJ4297 is a derivative of pSEK4 in which the *act*-PKS genes were replaced by a 3.8 kb *PacI*-*EcoRI* *whiE*-PKS fragment. *PacI* and *EcoRI* were introduced by cloning the 3.8 kb *Bam*HI-*NruI* fragment from pIJ4274 into pNEB193 (New England Biolabs). pIJ4298 is a derivative of pSEK4 in which

(35) Brown, D. W.; Hauser, F. M.; Tommasi, R.; Corlett, S.; Salvo, J. J. *Tetrahedron Lett.* **1993**, *34*, 419–422.

(36) Brown, D. W.; Salvo, J. J. *Appl. Environ. Microbiol.* **1994**, *60*, 979–983.

(37) Mayorga, M. E.; Timberlake, W. E. *Mol. Gen. Genet.* **1992**, *235*, 205–212.

(38) Bax, A.; Subramanian, S. *J. Magn. Reson.* **1986**, *67*, 565–569.

(39) Bax, A.; Summers, M. F. *J. Am. Chem. Soc.* **1986**, *108*, 2093–2094.

(40) Reynolds, W. F.; McLean, S.; Perpich-Dumont, M.; Enriquez, R. G. *Magn. Reson. Chem.* **1989**, *27*, 162–169.

(41) Hopwood, D. A.; Bibb, M. J.; Chater, K. F.; Kieser, T.; Bruton, C. J.; Kieser, H. M.; Lydiate, D. J.; Smith, C. P.; Ward, J. M.; Schrempf, H. *Genetic Manipulations of Streptomyces: A Laboratory Manual*; The John Innes Foundation: Norwich, 1985.

(42) Sambrook, J.; Fritsch, E. F.; Maniatis, T. *Molecular Cloning, a Laboratory Manual*; Cold Spring Harbor Laboratory Press: Cold Spring Harbor, NY, 1989.

(31) Fu, H.; McDaniel, R.; Hopwood, D. A.; Khosla, C. *Biochemistry* **1994**, *33*, 9321–9326.

(32) Alvarez, M. A.; Fu, H.; Khosla, C.; Hopwood, D. A.; Bailey, J. E. *Nat. Biotechnol.* **1996**, *14*, 335–338.

(33) A similar post-PKS reduction by a *S. coelicolor*-encoded dehydrogenase has recently been proposed to account for the observed ketoreduction of an eight-membered ring lactone generated from an engineered derivative of the 6-deoxyerythronilide B synthase. Kao, C. M.; McPherson, M.; McDaniel, R. N.; Fu, H.; Cane, D. E.; Khosla, C. *J. Am. Chem. Soc.* **1997**, *119*, 11339–11340.

(34) Perkins, E. J.; Gordon, M. P.; Caceres, O.; Lurquin, P. F. *J. Bacteriol.* **1990**, *72*, 2351–2359.

the *act*-PKS genes were replaced by a 4.2 kb *PacI*-*EcoRI* *whiE*-PKS fragment. *PacI* and *EcoRI* were introduced by cloning the 4.2 kb *Bam*HI-*Xmn*I fragment from pIJ4274 into pNEB193. pIJ4300 is a derivative of pSEK4 in which the *act*-PKS genes were replaced by a 4.6 kb *PacI*-*EcoRI* *whiE*-PKS fragment. *PacI* and *EcoRI* were introduced by cloning the 4.6 kb *Bam*HI-*Sph*I fragment from pIJ4274 into pNEB193. pIJ4301 is a derivative of pSEK4 in which the *act*-PKS genes were replaced by a 3.2 kb *PacI*-*EcoRI* *sch*-PKS fragment. *PacI* was introduced by cloning the 3.2 kb *Bsp*HI-*EcoRI* fragment from pUO6003^{3,7} into pT1. pIJ4302 is a derivative of pRM5 in which the *act*-PKS genes were replaced by a 3.2 kb *PacI*-*EcoRI* *sch*-PKS fragment. *PacI* was introduced by cloning the 3.2 kb *Bsp*HI-*EcoRI* fragment from pUO6003 into pT1. pIJ4303 is a derivative of pSEK4 in which the *act*-PKS genes were replaced by a 3.2 kb *PacI*-*EcoRI* *cur*-PKS fragment. *PacI* and *EcoRI* were introduced by cloning the 3.2 kb *Bsp*HI-*Sph*I fragment from pSB217⁶ into pT1. pIJ4304 is a derivative of pRM5 in which the *act*-PKS genes were replaced by a 3.2 kb *PacI*-*EcoRI* *cur*-PKS fragment. *PacI* and *EcoRI* were introduced by cloning the 3.2 kb *Bsp*HI-*Sph*I fragment from pSB217 into pT1. pIJ4305 is a derivative of pSEK4 in which the *act*-PKS genes were replaced by a 5.0 kb *PacI*-*EcoRI* *cur*-PKS fragment. *PacI* was introduced by cloning the 5.0 kb *Bsp*HI-*EcoRI* fragment from pSB217 into pT1.

Culture Conditions and Extraction. The strains were grown on R5⁴¹ agar plates (2 L) containing 5 μ g/mL thioestrepton at 30 °C for 1 week. The cultured agar was chopped and extracted with 80:15:5 EtOAc/MeOH/AcOH (2 L) at room temperature for 2 h. The organic solution was collected through filtration, and the remaining agar residue was extracted twice more as described above. The combined filtrates were concentrated under vacuum.

Isolation of TW93a–d (1–4) from *S. coelicolor* YU105/pIJ4293. The crude extract was subjected to C-18 silica gel (300 g) flash chromatography and eluted with 30% acetone in H₂O to give mixed fractions containing predominantly **1** and **2–4**. Final purification of **1** was achieved by reversed-phase HPLC on a 250 \times 22.5 mm C-18 column (Alltech Econosil) with 20% CH₃CN in 1% acetic acid (10 mL/min flow rate, 280/410 nm detection) to give TW93a (**1**, 8 mg) with a retention time of 16.5 min. **2–4** were purified by reversed-phase HPLC on a 300 \times 10 mm C-18 column with 25% CH₃CN in 1% acetic acid (4.5 mL/min flow rate, 280/410 nm detection) to give TW93b (**2**, 6.4 mg, *t*_R 13.1 min), TW93c (**3**, 20.3 mg, *t*_R 18.7 min), and TW93d (**4**, 10 mg, *t*_R 20.2 min). Similar amounts of **1–4** were detected in extracts of *S. coelicolor* YU105/pIJ4297, pIJ4301, and pIJ4303 by HPLC.

TW93a (1): UV λ_{\max} (ϵ) 216 (2550), 238 (1150), 282 (1050); IR (KBr) ν_{\max} 3412, 3179, 2925, 1684, 1676, 1600, 1590, 1452, 1444, 1355, 1264, 1169, 1024, 998; HRFABMS *m/z* 277.0718 (calcd for C₁₄H₁₃O₆, -0.6 mmu error); ¹³C NMR (125 MHz, CD₃OH) δ 32.5 (C14), 38.4 (C6), 89.5 (C2), 102.4 (C10), 102.9 (C4), 111.4 (C8), 120.8 (C12), 137.5 (C7), 160.7 (C11), 161.9 (C9), 167.0 (C5), 168.1 (C1), 173.8 (C3), 205.6 (C13); ¹³C NMR (125 MHz, CD₃OD) δ 32.5 (C14), 38.4 (C6), 89.0 (C2), 102.2 (C10), 102.8 (C4), 111.3 (C8), 120.8 (C12), 137.5 (C7), 160.5 (C11), 161.7 (C9), 167.0 (C5), 168.0 (C1), 173.4 (C3), 205.6 (C13); see Table 2 for additional NMR spectral data.

TW93b (2): UV λ_{\max} (ϵ) 214 (17 400), 244 (7250), 252 (6600), 294 (5000); IR (KBr) ν_{\max} 3410, 3142, 2922, 1670, 1632, 1625, 1566, 1440, 1353, 1343, 1253, 1166, 1023, 994; HRFABMS *m/z* 409.0912 (calcd for C₂₂H₁₇O₈, 1.1 mmu error); see Table 2 for NMR spectral data.

TW93c (3): UV λ_{\max} (ϵ) 216 (15 150), 288 (6600), 338 (2500); IR (KBr) ν_{\max} 3408, 3088, 2926, 1693, 1682, 1619, 1574, 1567, 1435, 1360, 1313, 1252, 1177, 1023, 990; HRFABMS *m/z* 465.0840 (calcd for C₂₄H₁₇O₁₀, -1.8 mmu error); see Table 2 for NMR spectral data.

TW93d (4): UV λ_{\max} (ϵ) 216 (19 950), 238 (10950), 284 (10000); IR (KBr) ν_{\max} 3428, 3180, 2923, 1702, 1664, 1660, 1618, 1608, 1508, 1459, 1275, 1166, 1025, 999; HRFABMS *m/z* 469.1122 (calcd for C₂₄H₂₁O₁₀, 1.3 mmu error); see Table 2 for NMR spectral data.

Isolation of TW94a–d (5–8) from *S. coelicolor* YU105/pIJ4294. The crude extract was chromatographed on a normal-phase silica gel (500 g) flash column and eluted with a stepwise chloroform to methanol

gradient to give mixed fractions containing predominantly **5–7** and **8**. Purification of **5–7** was achieved by reversed-phase HPLC on a 300 \times 10 mm C-18 column with a 30–70% CH₃CN in 1% acetic acid solvent gradient (30 min, 4.5/min mL flow rate, 280/410 nm detection) to give TW94a (**5**, 3 mg, *t*_R 11.1 min), TW94b (**6**, 9 mg, *t*_R 28.9 min), and TW94c (**7**, 5 mg, *t*_R 24.8 min). TW94d (**8**, 11 mg, *t*_R 21.9 min) was likewise purified by reversed-phase HPLC, but without the gradient. Similar amounts of **5–8** were detected in extracts of *S. coelicolor* YU105/pIJ4302 and pIJ4304 by HPLC.

TW94a (5): UV λ_{\max} (ϵ) 220 (2950), 284 (2700), 318 (1250); IR (KBr) ν_{\max} 3426, 3190, 2922, 1686, 1619, 1577, 1459, 1379, 1360, 1271, 1211, 1166, 1074, 1029, 999; HRFABMS *m/z* 167.0711 (calcd for C₉H₁₁O₃, -0.3 mmu error); see Table 4 for NMR spectral data.

TW94b (6): UV λ_{\max} (ϵ) 210 (28 850), 252 (10 500), 294 (6800), 328 (4250), 398 (3400), 414 (3250); IR (KBr) ν_{\max} 3425, 3074, 2921, 1676, 1606, 1578, 1468, 1413, 1387, 1346, 1308, 1257, 1182, 1169, 1114, 1048, 1021, 993; HRFABMS *m/z* 349.1056 (calcd for C₂₁H₁₇O₅, 2.0 mmu error); see Table 4 for NMR spectral data.

TW94c (7): [α]_D -14° (10 mg/mL, MeOH); UV λ_{\max} (ϵ) 212 (35 500), 284 (12 300), 338 (13 500), 374 (8500), 392 (10000), 414 (7250); CD $\Delta\epsilon_{228}$ -2.5, $\Delta\epsilon_{245}$ +0.19, $\Delta\epsilon_{262}$ -1.6, $\Delta\epsilon_{297}$ +3.0, $\Delta\epsilon_{320}$ -0.076, $\Delta\epsilon_{340}$ +1.3, $\Delta\epsilon_{367}$ -0.63; IR (KBr) ν_{\max} 3433, 2921, 1701, 1664, 1606, 1580, 1555, 1515, 1420, 1382, 1346, 1328, 1207, 1189, 1154, 1131, 1017; HRFABMS *m/z* 347.0908 (calcd for C₂₁H₁₅O₅, 1.1 mmu error); see Table 4 for NMR spectral data.

TW94d (8): UV λ_{\max} (ϵ) 214 (19 500), 236 (13 200), 286 (5350), 330, (4250), 388 (2550); IR (KBr) ν_{\max} 3404, 3087, 2924, 1693, 1672, 1619, 1567, 1496, 1435, 1378, 1313, 1252, 1177, 1124, 1105, 1023, 990; HRFABMS *m/z* 391.1161 (calcd for C₂₃H₁₉O₆, 2.1 mmu error); see Table 4 for NMR spectral data.

Isolation of TW95a,b (9,10) from *S. coelicolor* YU105/pIJ4295. The crude extract was chromatographed on a normal-phase silica gel (500 g) flash column and eluted with a stepwise chloroform to methanol gradient to give a pure fraction of TW95a (**9**, 100 mg) and an impure fraction containing **10**. Final purification of TW95b (**10**, 16 mg) was achieved by reversed-phase HPLC on a 250 \times 22.5 mm C-18 column with 35% CH₃CN in 1% acetic acid (10 mL/min flow rate, 280/410 nm detection, *t*_R 12.6 min) followed by Sephadex LH-20 using 90:10:0.1 MeOH/H₂O/AcOH as eluent. Similar amounts of **9** and **10** were detected in extracts of *S. coelicolor* YU105/pIJ4296, pIJ4298, and pIJ4305 by normal-phase TLC (10:1:0.5 CHCl₃/MeOH/AcOH).

TW95a (9): UV λ_{\max} (ϵ) 216 (41 700), 238 (35 500), 284 (24 550), 340 (9550), 404 (5250); IR (KBr) ν_{\max} 3229, 1672, 1621, 1589, 1560, 1447, 1383, 1334, 1247, 1165, 1101, 1006; HRFABMS *m/z* 451.1006 (calcd for C₂₄H₁₉O₉, 2.3 mmu error); see Table 6 for NMR spectral data.

TW95b (10): UV λ_{\max} (ϵ) 214 (26 350), 236 (18 600), 292 (19 950), 404 (3650), 492 (2100); IR (KBr) ν_{\max} 3412, 1685, 1618, 1575, 1480, 1448, 1414, 1247, 1174, 1100, 1022; HRFABMS *m/z* 465.0818 (calcd for C₂₄H₁₇O₁₀, 0.4 mmu error); see Table 6 for NMR spectral data.

Acknowledgment. We would like to thank Sheng Xiang Qiu, University of Illinois at Chicago, for acquiring NOE, HETCOR, and FLOCK NMR data for **6** and **9** and Dr. Michael Müller, University of Washington, for measuring the CD spectrum of **7**. This research was supported in part by the National Institutes of Health (AI 20264, H.G.F.), the National Science Foundation (MCB-9417419, C.K.), and the John Innes Foundation (D.A.H.).

Supporting Information Available: ¹H and ¹³C NMR spectra for **1–10**, HMBC spectra for **1–4**, **7**, and **10**, a HMQC spectrum for **4**, HETCOR spectra for **8** and **9**, a FLOCK spectrum for **9**, and a CD spectrum for **7** (32 pages, print/PDF). See any current masthead page for ordering information and Web access instructions.